

Trapped flux, diamagnetic shielding, and Meissner effect in a disk of $\text{YBa}_2\text{Cu}_3\text{O}_7$

M. A-K. Mohamed, J. Jung, and J. P. Franck

Department of Physics, University of Alberta, Edmonton, Alberta, Canada T6G 2J1

(Received 9 January 1989; revised manuscript received 7 February 1989)

The trapped flux, diamagnetic shielding, and Meissner effect in polycrystalline $\text{YBa}_2\text{Cu}_3\text{O}_7$ disks have been investigated by the measurement of the distribution of magnetic field across the sample at 77 K. The measurements were performed for samples cooled in zero and nonzero external magnetic fields. The distribution of the magnetic field was studied both in the presence of an applied magnetic field and when this field was switched off. The results show the relationship between shielding effect, Meissner effect, and flux pinning effect. Partial creep of flux into the disk was observed to occur for zero-field-cooled samples in applied magnetic fields as low as 1 G. The time decay of the trapped flux was observed to be logarithmic in time. The logarithmic decay rate increases linearly with the magnitude of the trapped magnetic field.

In this paper we present low-temperature experimental data on the magnetic field distribution measured across a disk-shaped sample of ceramic $\text{YBa}_2\text{Cu}_3\text{O}_7$ over an applied magnetic field range from 0.5 to 100 G. These data were taken for both the field-cooled and zero-field-cooled samples. The measurements of the Meissner effect in high-temperature superconductors^{1,2} show strong dependence of this effect on the magnitude of the applied magnetic field. Superconducting quantum interference device (SQUID) magnetometer data³ on ceramic and single-crystal Y-Ba-Cu-O show a remanent magnetic moment which is equal to the difference of the field-cooled and zero-field-cooled moments in the low-field, low-temperature range. The related Meissner fraction (field-cooled moment) was observed to change strongly with the applied field. These data were argued to point to conventional flux-pinning concepts⁴ in type-II superconductors rather than to a granular superconductive glass model. The results presented in this work show the direct relationship between the diamagnetic shielding effect, the Meissner effect, and the flux-pinning effect for both field-cooled and zero-field-cooled samples. We have studied the flux-creep phenomenon in these samples and its dependence on the magnitude of trapped flux. The magnetic field distribution in a sample was measured at 77 K with an axial cryogenic Hall probe (sensitivity ± 3 mG) which was scanned along the diameter of the disk-shaped sample. The area of the sensitive part of the probe was equal to 0.44 mm². The axial probe measured the component of the magnetic field perpendicular to a disk-shaped sample at the distance about 1 mm from the sample. The probe was connected to a gauss meter and a computer-controlled system, which also allowed measurements of fast trapped flux decays. A solenoid was used to generate a magnetic field which was applied in the direction perpendicular to the disk plane.

The sample of $\text{YBa}_2\text{Cu}_3\text{O}_7$ was prepared by standard solid-state reaction techniques from the metal oxides Y_2O_3 (99.99% purity), CuO (99.999% purity), and BaCO_3 (99.995% purity). The powders were mixed, ground, and formed into a pellet of diameter 16 mm and approximately 3 mm thick. Calcining was performed at

905 °C for 24 h in air. After reaction the pellet was re-ground, a new pellet was formed under a pressure of 7300 bar (diameter 16 mm, thickness about 2 mm) and sintered in flowing O_2 for 7 h at 925 °C. The compound was furnace cooled for 12 h at an initial rate of 200 °C/h. The average grain size was found to be within the range between 4 and 7 μm using scanning electron microscopy.

The measurement of a magnetic field distribution across the disk-shaped sample was performed for zero field cooling and field cooling. The experimental results for the zero-field-cooled sample are shown in Figs. 1(a)–1(h). The upper curves show magnetic field distributions measured across the disk while the external magnetic field over a range from 1 to 40 G was applied to the sample. Zero field cooling and subsequent application of a field show a diamagnetic shielding reaching 72.3% in a field of 1.7 G and decreasing down to 4.4% in a field of 39.0 G. The lower curves show the distribution of a trapped magnetic field measured across the disk after the external field was reduced to zero. The asymmetry observed for the trapped flux distribution is mainly due to the nonuniform microstructure of the sample. One can see from these graphs that the flux lines start to penetrate the disk from the perimeter towards its center at applied fields as low as 1 G. For applied fields over a range from 1 to 4.5 G, the flux lines are mostly pinned along the disk perimeter [Figs. 1(b)–1(e)]. It can be noticed that diamagnetic shielding of the disk is modified by the flux-pinning effect [Figs. 1(d) and 1(e)].

The experimental data for a disk-shaped sample cooled in an external magnetic field are shown in Figs. 2(a)–2(f). The upper curves show magnetic field distributions measured across the disk while the external magnetic field over a range from 0.5 to 50 G was applied to the sample. Field cooling shows the Meissner effect reaching 11.1% in the field 0.5 G and decreasing down to 2.2% in the field 48.0 G. The Meissner effect is stronger along the disk perimeter [Figs. 2(b)–2(e)]. The lower curves show distributions of the trapped magnetic field measured across the disk after the external field was reduced to zero. The flux lines are mostly pinned at the central part of the disk. It can be seen that the Meissner effect is modified by flux

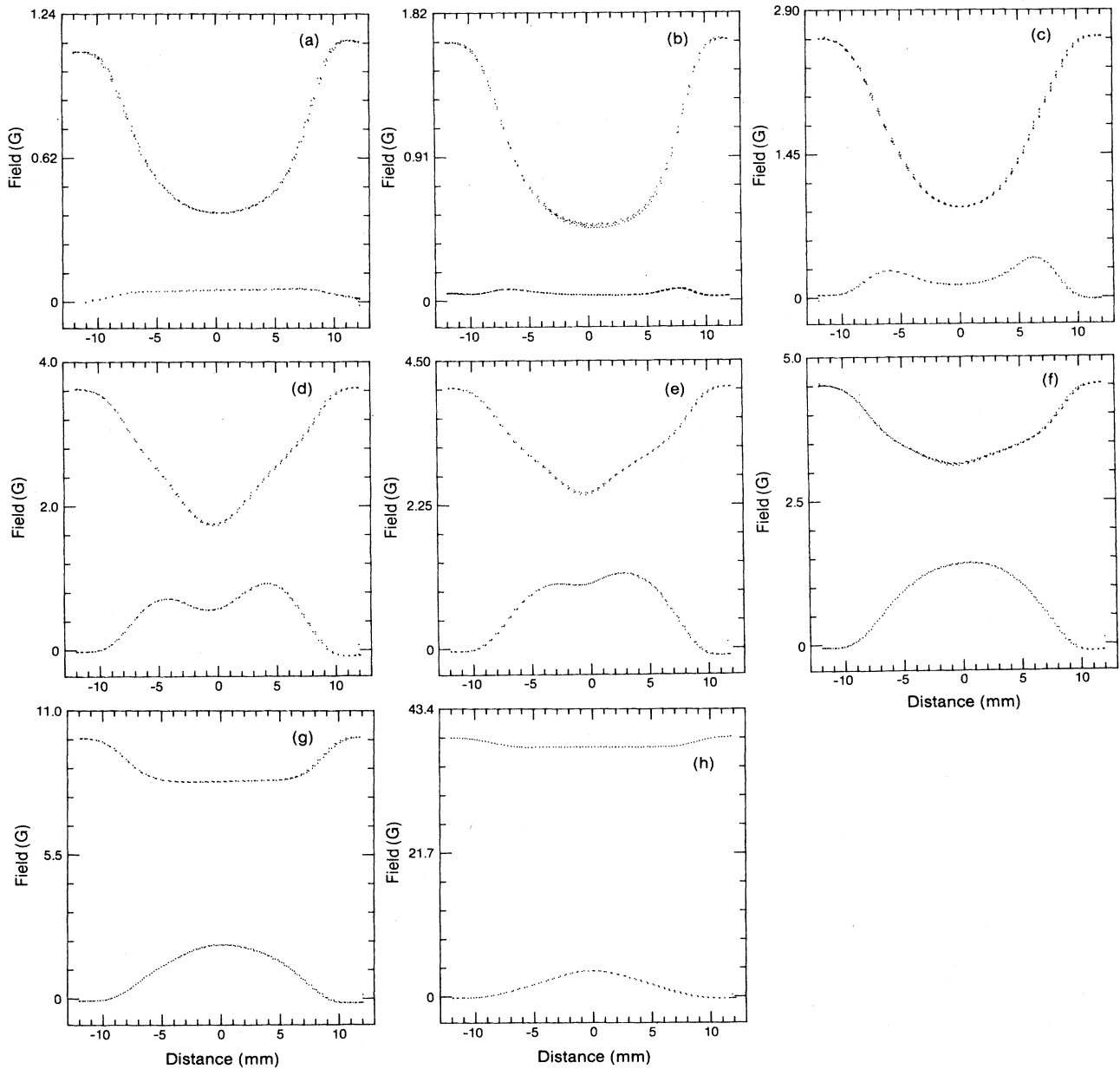


FIG. 1. Magnetic field distributions for a zero-field-cooled disk-shaped sample measured for different applied magnetic fields at 77 K: (a) 1.1 G; (b) 1.6 G; (c) 2.6 G; (d) 3.6 G; (e) 4.1 G; (f) 4.5 G; (g) 9.9 G; (h) 39.1 G. Upper curves show diamagnetic shielding (applied field present) reaching (at the center) (a) 66.7%; (b) 72.3%; (c) 66.7%; (d) 52.2%; (e) 41.1%; (f) 31.1%; (g) 16.7%; (h) 4.4%. Lower curves show a trapped field (applied field reduced to zero). Distances -8 and $+8$ mm mark the disk edges.

trapping. Figure 3 shows decays of trapped flux for a zero-field-cooled sample measured at the disk center. These decays are logarithmic in time, in good agreement with our earlier studies.⁵ The logarithmic decay rate is proportional to the magnitude of the trapped magnetic field (Fig. 4). Similar trapped field decays are also observed for the field-cooled sample. The dependence of the trapped field on applied magnetic field for both zero-field-cooled and field-cooled samples are shown in Fig. 5. The trapped field for a field-cooled sample achieves its sat-

uration value for applied fields above 20 G; however, for the zero-field-cooled sample, the trapped field reaches saturation at a magnetic field above 35 G.

The comparison of magnetic field distributions measured with an applied field present and when this field is reduced to zero (upper and lower curves in Figs. 1 and 2) indicates that for zero-field-cooled samples the diamagnetic shielding effect is reduced once flux lines are able to penetrate the material. Some flux penetration occurs at an applied field as low as 0.5 G. Figures 1(d) and 1(e)

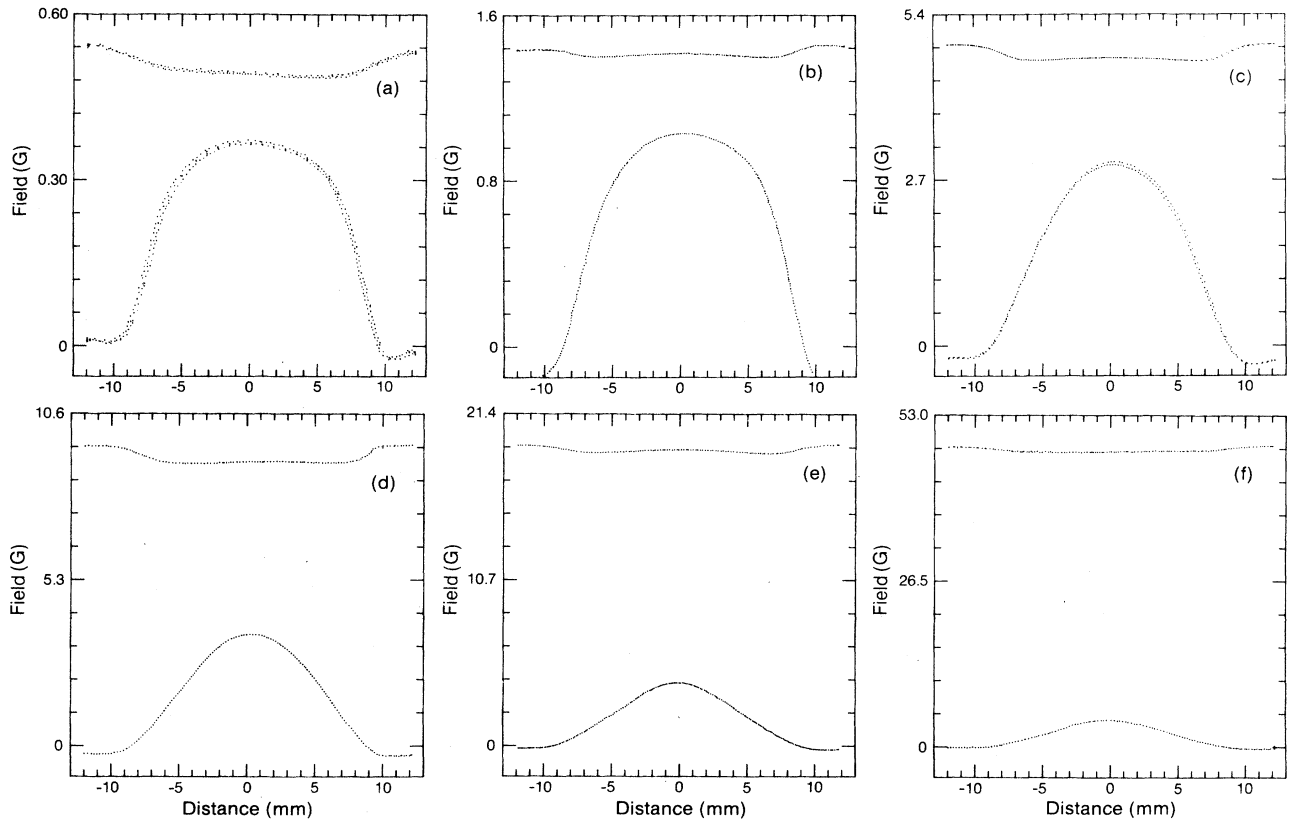


FIG. 2. Magnetic field distributions for a field-cooled disk-shaped sample measured for different applied magnetic fields: (a) 0.5 G; (b) 1.4 G; (c) 4.9 G; (d) 9.5 G; (e) 19.3 G; (f) 47.7 G. Upper curves show the Meissner effect (applied field present) reaching (a) 11.1%; (b) 3.3%; (c) 5.5%; (d) 5.6%; (e) 3.3%; (f) 2.2%. Lower curves show trapped field (applied field reduced to zero). Distances -8 and $+8$ mm mark the disk edges.

show clearly the change of the shielding effect in the sample due to flux-line creep into the disk along its perimeter, where the applied field gradient is the largest. This gradient is produced because of a shielding effect or large demagnetization effects at the edges of non-ellipsoid-

shaped samples, or by a combination of them. The demagnetizing factor of a flat disk could be responsible for the increase of field above H_{c1} at the edge of the disk.⁶ The flux creep in $\text{YBa}_2\text{Cu}_3\text{O}_7$ was also discussed by McHenry *et al.*⁷ In the flux creep model, flux bundles interact with shielding currents through the Lorentz force. When this force is larger than pinning forces, flux bundles are free to move through the material, experiencing only a viscous drag force due to the pinning centers.

The analysis of magnetic field distributions measured for field-cooled samples (Fig. 2) show that the Meissner

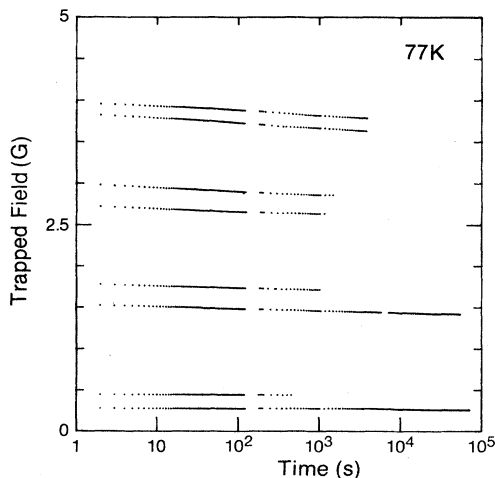


FIG. 3. Decays of a trapped magnetic field measured at the disk center for the zero-field-cooled case. The decays are logarithmic in time. Decays for the field-cooled case are similar.

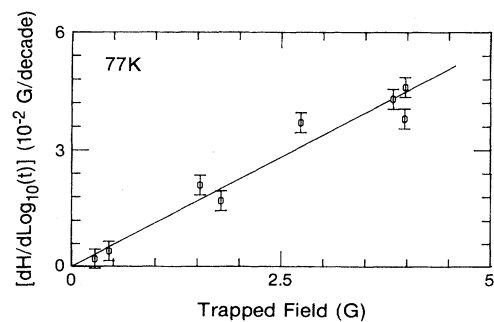


FIG. 4. The dependence of the logarithmic decay rate on the initial magnitude of trapped field.

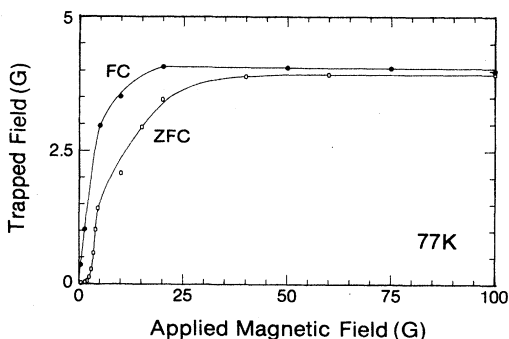


FIG. 5. The dependence of the trapped field on the applied magnetic field; open circles: zero-field-cooled sample; solid circles: field-cooled sample.

effect is much smaller than the diamagnetic shielding. Magnetic flux penetrating the disk center is not expelled upon cooling below T_c . The sample has both a Meissner contribution and a trapped flux that nearly cancel each other. According to the discussion presented by Maletta *et al.*,¹ at applied fields above 10 G, a larger flux gradient may overcome the trapping and thus cause larger fractional flux expulsion. Our results for applied fields at 20 and 50 G [Meissner effect 3.3% and 2.2%; Figs. 2(e) and 2(f)] do not suggest such behavior. The relationship between the Meissner effect and trapped flux was also discussed by Rennard *et al.*⁸ Their SQUID magnetometer data taken for a field-cooled ceramic Y-Ba-Cu-O sample showed the presence of two magnetic contributions of opposite sign, that were identified with the spatial distribution of screening currents and of pinned vortices.

The decays of the trapped field for both zero-field-cooled and field-cooled samples (Fig. 3) show logarithmic dependence with time, in good agreement with Anderson's flux-creep theory⁴ and the experimental results by Kim, Hempstead, and Strnad⁹ in type-II superconductors. We

have plotted $dH_{\text{trap}}/d \log_{10} t$ as a function of trapped field measured at $t=0$ (Fig. 4). The logarithmic decay rate is proportional to trapped magnetic field and also to the magnitude of the applied field. Logarithmic decays of the magnetization M as a function of time have been measured by Mota *et al.*¹⁰ in a zero-field-cooled sample of powdered $\text{La}_{1.8}\text{Sr}_{0.2}\text{CuO}_4$ at $T=4.2$ K and at $H_{\text{app}}=0$. The logarithmic decay rate $dM/d \ln t$ has been found to be proportional to H_{app}^n , where $3 < n < 4$. The sintered La-Sr-Cu-O specimen shows a deviation from this law ($n < 2$) for $H_{\text{app}} < 50$ G. This deviation was argued to be connected with the granular structure of sintered specimen. In sintered samples when H_{app} is reduced to zero, flux is trapped in the voids formed by grains joined by weak Josephson's junctions, causing additional contribution to the relaxation of magnetization.

The dependence of the trapped field on the applied field measured on a disk of $\text{YBa}_2\text{Cu}_3\text{O}_7$ (Fig. 5) agrees with Leiderer's results¹¹ for a broken ring of $\text{YBa}_2\text{Cu}_3\text{O}_7$ ceramic sample.

In conclusion, we have measured the field distribution across the diameter of a disk-shaped sample of ceramic $\text{YBa}_2\text{Cu}_3\text{O}_7$. The measurements were performed with an applied field on and off for both zero-field-cooled and field-cooled samples. The results demonstrate clearly the relationship between the diamagnetic shielding, Meissner effect, and flux-pinning phenomena. The magnitude of the trapped field was found to depend both on applied field and on sample-cooling conditions (i.e., zero field cooling or field cooling). Trapped flux becomes independent of these two factors for fields larger than 20–35 G, where it reaches a saturation value near 4 G. The trapped flux decays are logarithmic in time. The decay rates depend linearly on the initial magnitude of trapped field.

This work has been supported by grants from the Natural Sciences and Engineering Council of Canada.

¹H. Maletta, A. P. Malozemoff, D. C. Cronmeyer, C. C. Tsuei, R. L. Greene, J. G. Bednorz, and K. A. Müller, *Solid State Commun.* **62**, 323 (1987).

²T. R. McGuire, T. R. Dinger, P. Freitas, W. J. Gallagher, T. S. Plaskett, R. L. Sandstrom, and T. M. Shaw, *Phys. Rev. B* **36**, 4032 (1987).

³A. P. Malozemoff, L. Krusin-Elbaum, D. C. Cronmeyer, Y. Yeshurun, and F. Holtzberg, *Phys. Rev. B* **38**, 6490 (1988).

⁴P. W. Anderson, *Phys. Rev. Lett.* **9**, 309 (1962).

⁵M. A-K. Mohamed, W. A. Miner, J. Jung, J. P. Franck, and S. B. Woods, *Phys. Rev. B* **37**, 5834 (1988).

⁶D. Schoenberg, *Superconductivity* (Cambridge Univ. Press,

Cambridge, 1952), p. 22.

⁷M. E. McHenry, M. Foldeaki, J. McKittrick, R. C. O'Handley, and G. Kalonji, *Physica C* **153-155**, 310 (1988).

⁸J. P. Rennard, C. Giovanella, L. Fruchter, and C. Chappert, *Physica C* **153-155**, 330 (1988).

⁹Y. B. Kim, C. F. Hempstead, and A. R. Strnad, *Phys. Rev. Lett.* **9**, 306 (1962).

¹⁰A. C. Mota, A. Pollini, P. Visani, K. A. Müller, and J. G. Bednorz, *Phys. Rev. B* **36**, 4011 (1987); *Physica C* **153-155**, 67 (1988).

¹¹P. Leiderer and R. Feile, *Z. Phys. B* **70**, 141 (1988).